A Nd:YAG Laser-Pumped Hydrogen Raman Shifter with Capillary Waveguide

Maria Leilani Y. Torres*, Marilou M. Cadatal, and Wilson O. Garcia

Photonics Research Laboratory
National Institute of Physics, College of Science
University of the Philippines, Diliman, 1101 Quezon City
Telefax: (632)920-5474
E-mail: mltorres@nip.upd.edu.ph

ABSTRACT

Operation of a 355/532 nm Nd:YAG laser-pumped hydrogen Raman shifter with capillary waveguide (CWG) is demonstrated. For both pump wavelengths, more laser lines are generated using the Raman shifter with CWG compared to a conventional Raman shifter. Both 355 and 532 nm pumps showed a 60% decrease in threshold power for the generated first Stokes (S1) Laser line. The 355 nm-pumped Raman shifter with CWG generated S1 at 2.1 mW pump power at a hydrogen pressure of 1.38 MPa. On the other hand, for the 532 nm pumped waveguide Raman shifter at a hydrogen pressure of 1.72 MPa, the threshold power for S1 is at 8.3 mW. In addition, an improvement of the output powers is observed for the Stokes and anti-Stokes generated by Raman shifter with CWG.

Keywords: waveguide, stimulated Raman scattering

INTRODUCTION

The hydrogen Raman shifter is an efficient simple and economical method of simultaneously generating multiple laser lines. It has been used as a light source for two-photon two-color excitation studies (Palero et al., 2002) and pulsed color digital holography (Almoro et al., 2004). The Raman shifter utilizes a nonlinear phenomenon known as stimulated Raman scattering, which extends the tuning range of lasers into the vacuum ultraviolet (VUV) and to the far infrared (FIR) (Papayanis et al., 1998). Of the possible Raman medium, hydrogen is by far the most widely used due to its large Raman shift and high Raman transition probability leading to efficient shifting (Bhagavantam,

1942). However, SRS requires high pump intensity to reach its threshold (Benabid et al., 2002).

Several techniques such as high-finess Fabry Perot resonator (Benabid et al., 2002), multiple pass configurations and beam guidance with hollow dielectric waveguides (HDW) (Rabinowitz et al., 1976), and hollow core photonic crystal fibers (Benabid et al., 2002) have been utilized to achieve lower SRS threshold intensity. Classified as HDW (Marcuse,1974), capillary waveguides (CWG) are inexpensive tools to confine the gas and provide beam guidance. With the CWG inside the Raman shifter, an improvement of the conversion efficiency is achieved.

Developing a method to achieve low threshold intensity for SRS provides an avenue for numerous applications
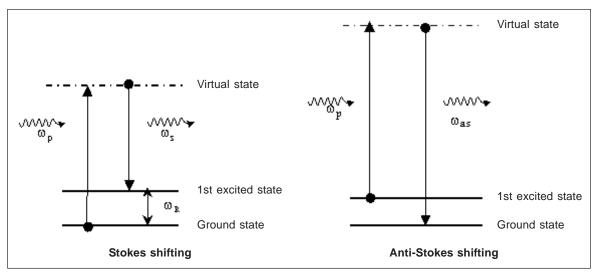
---

*Corresponding author

Fig. 1. An illustration of the frequency shifts due to the Raman effect.

in nonlinear optics and technology such as spectroscopy, remote sensing, and atomic physics (Benabid et al., 2002). Low threshold intensity of SRS can provide a light source suitable for image sectioning via multi-color multi-photon fluorescence microscopy, without damaging biological samples (Palero et al., 2002). With low pump beam intensity requirement, laser pump sources with lower output intensity can also be utilized. A further advantage of achieving a low threshold is that the available pump power can be divided to drive a Raman oscillator and amplifier. This configuration can result in a more efficient channeling of the pump power to generate the intended Stokes radiation (Berry et al., 1982).

In this paper, we compare the performances of a conventional Raman shifter and a Raman shifter with CWG using the 532 and 355 nm output of a Nd:YAG laser as pump beam in terms of the number of Raman components generated and threshold powers. Similarly, we investigate the dependence of output power of the Raman components with the hydrogen Raman pressure and input power.

Stimulated Raman scattering in capillary waveguide

The basic theory behind SRS is called the Raman effect. An illustration of the frequency shifts involved in Raman effect is shown in Fig. 1. A pump photon

interacts with a molecule in the ground state and excites it to a virtual state. When the molecule relaxes, it produces a photon of lower frequency compared to the pump photon. This shifted photon is called the Stokes (S) photon. On the other hand, when a molecule initially in the first excited state absorbs a pump photon and is excited to a higher virtual state, a photon of higher frequency to the pump photon is emitted when it relaxes spontaneously. This photon of higher frequency is known as the anti-Stokes (AS) photon.

SRS occurs when a sufficiently intense light beam interacts with a Raman medium to produce coherent radiation. Furthermore, when the first Stokes (S1) attains sufficient intensity, it may act as pump photon to produce higher order second Stokes (S2) and third Stokes (S3) lines as shown in Fig. 2. This process is known as the SRS cascade. Another nonlinear phenomenon known as the four-wave Raman mixing (FWRM) is also involved in the generations of the anti-Stokes and higher-ordered Stokes lines. FWRM is depleted at higher pressures due to an increase in wave vector mismatch (Shoulepnikoff,1997).

Conventional Raman shifters use a lens to focus the pump beam inside a gas cell. The nonlinear phenomena such as SRS and FWRM occur in the focal region known as the interaction region where the threshold for SRS to occur is achieved. This technique requires high input intensity for SRS to occur (Benabid et al., 2002).

With the use of a CWG inside the Raman shifter, the pump beam is confined and propagated by multiple grazing reflections (Verdeyen, 1981) which are equivalent to periodical focusing by a series of lenses (Arnaud, 1976) as shown in Fig. 3. This introduces foci along the hollow bore of the CWG. In effect, the length of interaction, z, between the pump and the medium increases.

According to Eq. (1), which gives the Stokes intensity, $I_s(z)$ (Papayanis et al., 1998), the increase in z will decrease the SRS threshold of the device and increase the conversion efficiency of the Raman lines:

$$I_s(z) = I_s(0)\exp\left(I_p(0)g_r z\right). \tag{1}$$

Here $I_p(0)$ is the pump beam intensity and g_r is the steady state Raman gain. The g_r is proportional to the Raman active gas pressure. Moreover, g_r is observed to saturate at high pressures (Schoulepnikoff et al.,
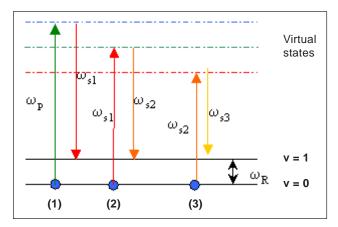

Fig. 2. Generation of (1) S1, (2) S2, and (3) S3 by SRS cascade.
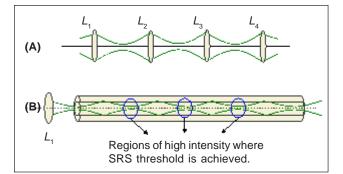

Fig. 3. The (B) propagation of light inside the capillary waveguide can be simulated by the focusing of light by (A) a series of lenses.

1997). In addition, a longer region of interaction provides longer region where phase matching between wave vectors can be satisfied. Hence, the effect of four-wave Raman mixing (FWRM) becomes prevalent.

Under steady-state conditions and for a focused single-mode pump laser, the Stokes power will grow as $\exp(G)$ where the cumulative gain coefficient G is given by

$$G = \frac{4g_R P_p \tan^{-1}\left(\frac{l}{b}\right)}{\lambda_S + \lambda_P}. \tag{2}$$

Here P_P is the laser pump power, λ_S and λ_P are the Stokes and pump wavelengths, respectively, and b is the confocal parameter (Perrone et al., 1997). According to Eq. (2), higher pump laser wavelengths lead to higher threshold energies and lower Stokes conversion efficiencies.

METHODOLOGY

The schematic diagram of the experimental setup is shown in Fig. 4. The laser pump is a Q-switched neodymium-doped yttrium-aluminum garnet (Nd:YAG) laser (Spectra Physics GCR-230) operating at 10 Hz repetition rate. The 1064 nm fundamental output is converted to its second (532 nm) and third (355 nm) harmonics using potassium dideuterium phosphate (KDP) crystals with pulse width of 5-6 ns. The mirrors M_1 and M_2 steers the beam into the setup. The pump beam passes through a diaphragm D and expanded using a telescope. A 1 mm aperture A approximates a plane wave and lens L_1 ($f = 290$ mm) focuses the beam into a 50-cm long, 1 mm bore diameter silica glass (index of refraction ~1.5) capillary waveguide inside a 58-cm long Raman cell. The Raman cell consists of a pressurized stainless steel chamber made with both ends fitted with fused silica optical windows for laser beam input and output. After evacuating with a mechanical pump, it is filled with ultra high purity hydrogen (Cryogenic Rare Gas, 99.9999% purity) with pressure up to 4.14 MPa. The CWG is placed on top of a sheet of stainless steel made to fit the walls of the Raman cell. Lens L_2 collimates the beam into a Pellin broca prism (PB) which separates the Raman output into its components. The spectral characterization of the pump, Stokes, anti-Stokes, and
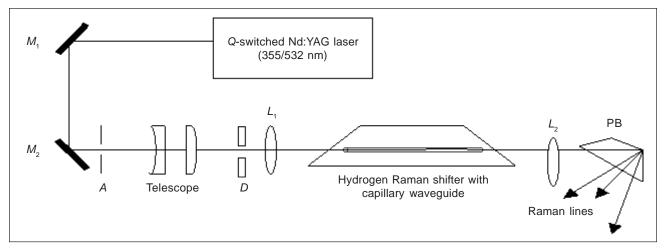
Fig. 4. Experimental setup for the generation of Raman lines, where M_1 and M_2–mirrors, A–aperture, D–diaphragm, L_1–focusing lens, L_2–collimating lens, and PB–Pellin Broca prism.

Rayleigh is executed using a computer-controlled monochromator (SPEX 1000M). The separated Raman components are placed incident to an optical fiber bundle input connected to the grating monochromator. Output powers are measured using a Melles-Griot broadband power meter. The CWG is removed from the Raman shifter for the operation of the conventional Raman shifter.

RESULTS AND DISCUSSION

355 nm pump beam

The spectral profile of the generated Raman components for a 355 nm pump beam is shown in Fig. 5(A) for the Raman shifter with CWG and Fig.5(B) for the conventional Raman shifter. Maximum number of five (5) Raman lines, three (3) Stokes, and (2) anti-Stokes lines with wavelengths ranging from 273.8 to 635.9 nm are generated using a Raman shifter with CWG at H_2 pressure = 1.38 MPa and input power (P_{in}) = 26.5 mW. Only two (2) Raman components S1 and S2 with wavelengths 415.9 and 502.9 nm, respectively, are generated via a conventional Raman shifter. The generation of the anti-Stokes lines in Fig. 5(A) shows the enhancement of the FWRM process in the presence of the CWG.

The dependence of the output power with H_2 pressure is shown in Fig. 6 for the conventional Raman shifter

and for the Raman shifter with CWG at P_{in} = 26.5 mW. In the presence of a CWG, the Rayleigh, otherwise known as the depleted pump rapidly decreases with increasing pressure due to its conversion to Raman components. On other hand, S1 and S2 increase with increasing pressure then saturate at H_2 pressure ≥ 2.76 MPa. This is due to the saturation of the H_2 Raman gain at high pressures (Schoulepnikoff et al., 1997). Higher output power can be observed for the Raman lines with CWG. S2 generated with CWG shows an improvement in its output powers with peak power of 1.3 mW at H_2 pressure = 3.45 MPa compared to only 0.03 mW without CWG. Interestingly, the output powers of S1 and the other Raman lines are exceeded by the output powers of S2 generated with CWG at pressures 2.07-3.05 MPa. S2 is primarily generated from S1 by SRS cascade. However, S1 is also utilized to generate anti-Stokes lines by FWRM. Because the output power of S1 is expended to generate not only higher ordered Stokes but anti-Stokes as well, S2 has a higher output power compared to S1. This is due to the longer interaction region provided by the CWG, which enhances FWRM and SRS cascade.

S1 is observed to have the same peak power of 1.5 mW at H_2 pressure = 0.69 MPa for the Raman shifter with CWG and H_2 pressure = 3.79 MPa for the conventional Raman shifter. This is in accordance with Eq. (1), where at the same pump power with shorter z, a higher g_r and hence a higher pressure must be attained.
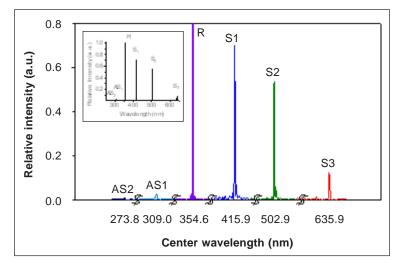
Fig. 5(A). Spectral profile of the Raman components generated from a Raman shifter with CWG at 26.5 mW input power and 1.38 MPa hydrogen pressure. Inset shows the actual location of the Raman lines. Intensity of Raman lines is normalized with respect to the Rayleigh.
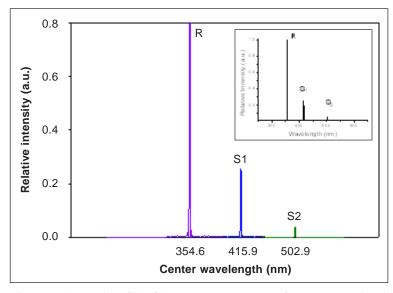

Fig. 5(B). Spectral profile of the Raman components from a conventional Raman shifter at 26.5 mW input power and 1.38 MPa hydrogen pressure. Inset shows the actual location of the Raman lines. Intensity of Raman lines is normalized with respect to the Rayleigh.

Figure 7 shows the dependence of the output power with pump power for the conventional and the Raman shifter with CWG operating at H_2 pressure =1.38 MPa. A threshold power is observed for the Raman lines. With increasing P_{in}, more Raman lines are generated. The threshold power of the Raman components with and without CWG is summarized in Table 1. At H_2 pressure = 1.38 MPa, S1 is generated at P_{in} = 2.1 mW for a Raman shifter with CWG compared to the

threshold power of S1 at P_{in} = 5.2 MPa generated without the waveguide. With the aid of CWG, the threshold power for S1 is reduced by 60% at of H_2 pressure = 1.38 MPa.

532 nm pump beam

Figure 8 shows the spectral profile of the generated Raman lines for a 532 nm pump beam with [Fig. 8(A)]
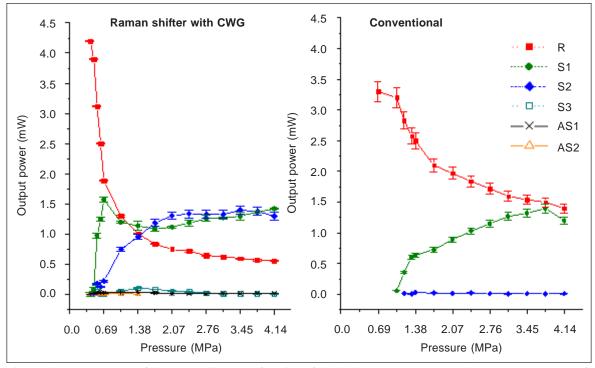
Fig. 6. The output power of the Raman lines as a function of the hydrogen gas pressure at 355 nm pump power of $P_{in} = 26.4$ mW with and without a capillary waveguide.
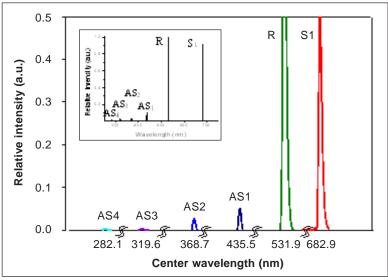

Fig. 7. The output power of Raman lines as a function of the 355 nm P_{in} at H_2 pressure of 1.38 MPa with and without a CWG.

	Threshold power (mW)				
	S1	S2	S3	AS1	AS2
With CWG	2.1	2.5	5.1	4.2	11.3
Without CWG	5.2	6.5	-	-	-

Table 1. Threshold power for the generated Raman components with and without CWG at H_2 pressure = 1.38 MPa for the 355 nm pump beam. Without CWG only S1 and S2 are generated.
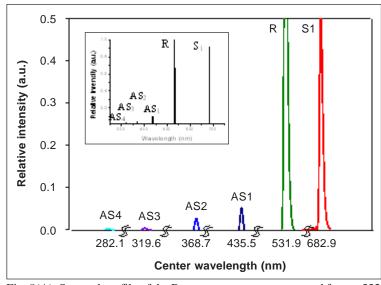
Fig. 8(A). Spectral profile of the Raman components generated from a 532 nm pumped Raman shifter with CWG at P_{in} = 46.5 mW and H_2 pressure =1.72 Mpa. Inset shows the actual location of the Raman lines. Intensity of the Raman lines are normalized with respect to the Rayleigh.
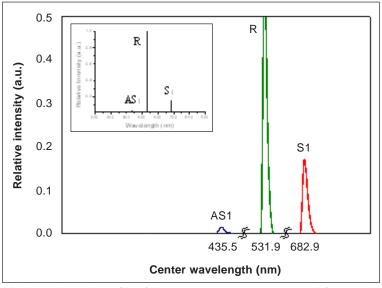

Fig. 8(B). Spectral profile of the Raman components generated from a 532 nm pumped Raman shifter without a CWG at P_{in} = 46.5 mW and H_2 pressure =1.72 MPa. Inset shows the actual location of the Raman laser lines. The intensities of the Raman lines are normalized with respect to the Rayleigh.

and without CWG [Fig. 8(B)]. With a CWG, five (5) Raman lines, S1 (682.9 nm), AS1 (435.5 nm), AS2 (368.7 nm), AS3 (319.6 nm), and AS4 (282.1 nm) are generated at H_2 pressure = 1.72 MPa and P_{in}= 46.5 mW. At the same H_2 pressure and P_{in}, the conventional Raman shifter generated only two (2) Raman lines, S1 and AS1. With the longer interaction region provided by the CWG, phase-matching between interacting wave vectors is improved. Hence, the enhancement of FWRM as manifested by the production of more anti-Stokes lines for a Raman shifter with CWG.

The dependence of output power with H_2 pressure is shown in Fig. 9. With CWG, S1 reaches its peak output
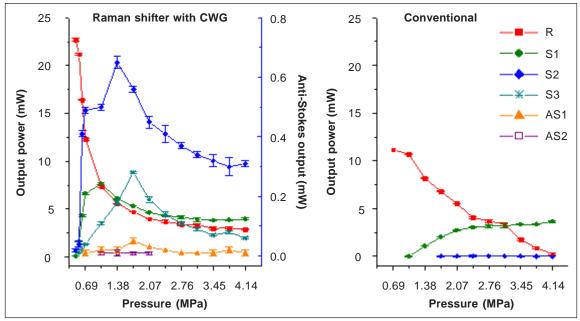
Fig. 9. The power of various Raman lines as a function of the H_2 pressure at 532 nm pump power of $P_{in} = 46.5$ mW with and without a capillary waveguide.
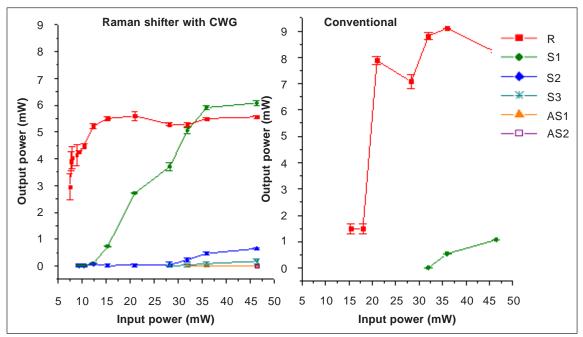

Fig. 10. The power of various Raman lines as a function of the 532 nm pump power at H_2 $P = 1.38$ MPa with and without a capillary waveguide.

| | Threshold power (mW) | | | | |
	S1	AS1	AS2	AS3	AS4
With CWG	8.3	9.5	19.1	46.3	46.5
Without CWG	21	36	-	-	-

Table 2. Threshold power of the Raman components generated from a 532 nm pumped H_2 Raman shifter with and without CWG at H_2 pressure = 1.72 MPa. Without CWG only S1 and AS1 are generated.

power at H_2 pressure =1.04 MPa and saturates at higher pressures due to the saturation of the H_2 Raman gain. The output power of the AS1 generated from the Raman shifter with CWG reaches its peak at H_2 P = 1.38 MPa. At midrange H_2 pressure (1.38-2.07 MPa), FWRM is most efficient. Hence, higher output power is attained by the anti-Stokes lines are at this pressure range. At H_2 pressure $\geq$ 2.07 MPa, the AS lines are rapidly depleted since it is difficult to satisfy phase matching conditions at high pressures. Higher output powers are achieved for the Raman lines generated by the Raman shifter with CWG.

Figure 10 shows plots of the output powers of the Raman lines from the Raman shifter with CWG and the conventional Raman shifter as functions of P_{in}. As with the 355 nm pump beam, there is a threshold power to generate SRS. The threshold power of the Raman components is summarized in Table 2. However, because of lower cumulative gain G for longer pump wavelengths, higher threshold power can be observed using a 532 nm compared to a 355 nm pump beam. At H_2 pressure = 1.72 MPa, the threshold power for S1 generated from a Raman shifter with CWG is 8.1 mW. With longer interaction region, the threshold power of the device decreases.

CONCLUSION

Operation of a hydrogen Raman shifter with capillary waveguide is demonstrated. For a 355 nm pump beam, S1 is generated at 2.1 mW at H_2 pressure = 1.38 MPa while for the 532 nm-pump beam it is generated at 8.3 mW at H_2 pressure = 1.72 MPa. With the presence of CWG for the 355 nm excitation wavelength, S2 is observed to generate higher power compared to S1 and other Raman lines. More anti-Stokes lines are observed for a 532-nm pumped Raman shifter with CWG. For both pump wavelengths, a 60% reduction in threshold power is achieved. With a CWG, more Raman lines are generated and effects of FWRM are enhanced.

ACKNOWLEDGMENTS

REFERENCES

Almoro, P., M. Cadatal, W. Garcia, and C. Saloma, 2004. Pulsed full-color digital holography with a hydrogen Raman shifter. *Appl. Opt.* 43: 2267-2271.

Arnaud, J., 1976. Beam and fiber optics. Bell Tel. Labs, Inc.

Berry, A.J., D.C. Hanna, and D.B. Hearn, 1982. Low threshold operation of a waveguide H2 Raman laser. *Opt. Commun.* 43: 229-232.

Benabid, F., J.C. Knight, G. Antonopoulos, and P. Russel, 2002. Stimulated Raman scattering in hydrogen-filled hollow-core photonic crystal fiber. *Science*. 298: 399-402.

Bhagavantam, S., 1942. Scattering of light and the Raman effect. Chemical Publishing Company, New York.

Garcia, W.O., 2002. Temporal coherence control of a *Q*-switched frequency tripled (355 nm) Nd:YAG pumped hydrogen Raman shifter. Ph.D. dissertation, University of the Philippines.

Mannik, L. & S.K. Brown, 1986. Tunable infrared generation using third Stokes output from a waveguide Raman shifter. *Opt. Commun.* 57: 360-364.

Marcuse, D.,1974. Theory of dielectric optical waveguides. Bell Tel. Labs, Inc.

Palero, J., W. Garcia, and C. Saloma, 2002. Two-color (two-photon) excitation fluorescence with two confocal beams and a Raman shifter. *Opt. Commun.* 211: 57-63.

Papayannis, A., G. Tsikrikas, and A. Serafetinides, 1998. Generation of UV and VIS laser light by stimulated Raman scattering in H_2, D_2, and H_2/He using a pulsed Nd:YAG laser at 355 nm. *Appl. Phys. B*. 67: 563-568.

Perrone, M.R. *et al*., 1997. Dependence of rotational and vibrational Raman scattering on focusing geometry. *IEEE J. Quantum Electron.* 33: 6.

Schoulepnikoff *et al*., 1997. Experimental investigation of high-power single-pass Raman shifters in the ultraviolet with Nd:YAG and KrF lasers. *Appl. Opt*. 36: 5026-5043.

Verdeyen, J., 1981. Laser electronics. Prentice Hall, Inc., Englewoods Cliff, New Jersey.